Long-range electron-hole exchange interaction in aluminum nitride

Ryota Ishii ⬤,[*] Mitsuru Funato, and Yoichi Kawakami

Department of Electronic Science and Engineering, Kyoto University, Kyoto 615-8510, Japan

To resolve the discrepancies in the exciton fine structure of aluminum nitride (AlN), polarization- and angle-resolved photoluminescence (PL) spectroscopies are performed. The excitonic PL spectra strongly depend on the optical polarization and detection angle. We propose that both the long-range and short-range electron-hole exchange interaction should be used to interpret the luminescence spectra. The theoretical framework fully explains the present and previous experimental results. The large longitudinal-transverse splitting energy obtained in this study suggests that AlN has strong light-matter coupling without quantum-confined structures.

Solid-state light sources in the deep-ultraviolet (DUV) spectral region have attracted much attention for diverse applications. These include gas (e.g., NO_x) sensing, virus inactivation, fluorescence microscopy, and water purification [1–3]. However, the performance of DUV light-emitting diodes and laser diodes is low compared to that of visible ones [1,4,5]. Because the active layer of DUV light-emitting devices is composed of aluminum gallium nitride (AlGaN), which is an alloy of gallium nitride (GaN) and aluminum nitride (AlN), the optoelectronic properties of GaN and AlN should be thoroughly understood to enhance the performance of DUV light-emitting devices.

In this study, we focus on the intrinsic physics of excitons in AlN. Although the intrinsic excitonic properties of GaN are well understood [6–8], the exciton fine structure of AlN remains controversial. Figure 1 shows the excitonic photoluminescence (PL) spectrum of a *c*-plane homoepitaxial AlN film at 10 K. The 6.0112 eV peak is assigned to the optical transition of an exciton bound to a neutral donor silicon [9]. We proposed that the 6.0267- and 6.0399-eV peaks originate from the optical transition of a free exciton with irreducible representations of Γ_5 and Γ_1, respectively [10]. Some studies support our assignment [11–15]. On the other hand, Feneberg *et al.* proposed that the 6.0267-eV peak originates from a neutral donor-bound-exciton transition and the 6.0399-eV peak is due to a free exciton with the irreducible representation of Γ_5 [16]. Other studies support their assignment [17–20]. In addition to this discrepancy, nonpolar and semipolar plane AlN samples exhibit lower PL peak energies than those for *c*-plane AlN [16,21]. These behaviors cannot readily be explained by the difference of the residual strain. To address these issues and the origin of the 6.0306-eV peak, this study performs polarization- and angle-resolved PL spectroscopy for AlN. The experimental results can be explained by considering both the long-range and short-range electron-hole exchange interaction in AlN.

We employed two samples. The first one was a *c*-plane homoepitaxial AlN film grown by metal-organic vapor phase epitaxy on an AlN bulk substrate. The screw and edge dislocation densities were 1×10^5 cm^{-2} and $<4 \times 10^5$ cm^{-2}, respectively. The carbon concentration in the epilayer was below the detection limit of secondary ion mass spectroscopy, which is $<3 \times 10^{17}$ cm^{-3}. The oxygen and silicon concentrations were near the detection limit of 6×10^{17} cm^{-3} and 1×10^{16} cm^{-3}, respectively. Pretreatment of the substrate and the growth conditions are detailed elsewhere [22]. The second sample, an *m*-plane bulk AlN, was synthesized by a physical vapor transport method (purchased from CrystAl-N). Although the impurity concentrations were not evaluated, the PL spectra indicated relatively high impurity concentrations compared to those in the first sample. The effect of the residual strain difference between the samples can be neglected because we set the emission energy from a neutral donor-bound exciton at 6.0112 eV. (The binding energy of the donor-bound exciton is assumed to be strain-independent.)

Polarization- and angle-resolved PL spectroscopies were performed using a pulsed ArF excimer laser ($\lambda = 193$ nm). A linear-polarizer (DUVGT-15, Kogakugiken) was used for the polarization-resolved PL measurements. For angle-resolved PL measurements, detection optics with an acceptance angle of $6.9°$ were mounted on a rotating optical bench and the following luminescence signals were guided to the entrance slit of a monochromator by a solarization-resistant optical fiber. The PL signals were dispersed by a 50-cm monochromator with a LN$_2$-cooled charge-coupled device. The spectral resolution exceeded 0.045 nm at a wavelength of 200 nm, which corresponds to about 1 meV. The sample was loaded in a closed-cycle conduction-cooling cryostat. All the PL measurements were performed under a weak excitation condition (linear response regime).

Before describing the experimental results, the excitonic structure of AlN should be recalled [10]. Wurtzite crystals (e.g., AlN, GaN, and ZnO) have crystal symmetry belonging to the C_{6v} point group. The irreducible representations of the 1*s* exciton are written as $2\Gamma_1 \oplus 2\Gamma_2 \oplus 3\Gamma_5 \oplus \Gamma_6$. Γ_1 (singly degenerated) and Γ_5 (doubly degenerated) are dipole-

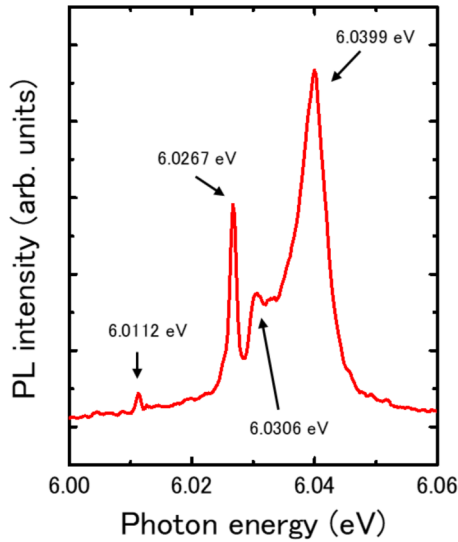*ryota.ishii@optomater.kuee.kyoto-u.ac.jp

FIG. 1. PL spectrum of a *c*-plane homoepitaxial AlN film at 10 K. The excitation power density is 19 kW/cm^2. There is no consensus on the origin of the 6.0267, 6.0306, and 6.0399 eV peaks.

allowed states for $E \parallel c$ and $E \perp c$, respectively. E and c are the electric field and the *c*-axis, respectively. Γ_2 (singly degenerated) and Γ_6 (doubly degenerated) are dipole-forbidden states. GaN and ZnO have a positive crystal-field splitting energy [8,23] while AlN has a huge negative crystal-field splitting energy [11]. Consequently, the *A* exciton (composed of the crystal-field split-off hole in AlN) has irreducible representations of $\Gamma_1 \oplus \Gamma_2 \oplus \Gamma_5$. The exciton binding energy of AlN ranges from 52 to 67 meV [14,24,25].

Figure 2 shows the polarization-dependent PL spectra of a *c*-plane homoepitaxial AlN film at 10 K when the sample was excited from the surface normal and the PL signal was detected at an angle of 60° from the surface normal. The
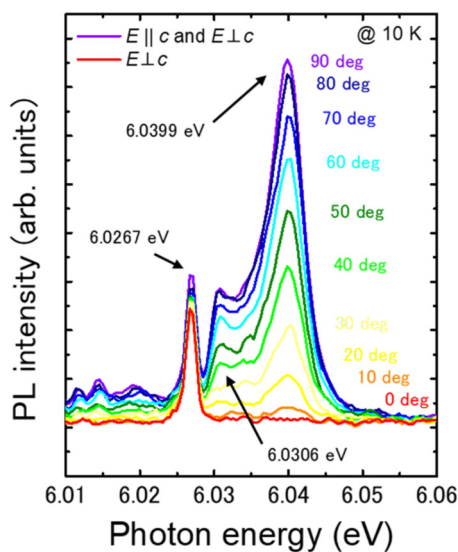

FIG. 2. Polarization-dependent PL spectra of a *c*-plane homoepitaxial AlN film at 10 K. The excitation power density is 72 kW/cm^2. The 6.0267-eV peak has an optical polarization of $E \perp c$ whereas the 6.0306 and 6.0399 eV peaks have an optical polarization of $E \parallel c$.

angles in Fig. 2 represent the tilt angle of the linear-polarizer. An angle of 0° corresponds to $E \perp c$. The $E \parallel c$ component increases as the angle increases. The 6.0267-eV peak appears regardless of the tilt angle, indicating that the peak has an optical polarization of $E \perp c$ and an irreducible representation of Γ_5. This is consistent with our previous studies [10,22]. Figure 2 also indicates that the 6.0306 and 6.0399 eV peaks have an optical polarization of $E \parallel c$. Hence, the two emission peaks have an irreducible representation of Γ_1 [10].

Next, angle-resolved PL spectroscopy was performed for a *c*-plane homoepitaxial AlN film. Figure 3(a) shows the experimental setup. The detection (external) angle ϕ is defined by the inclination angle of the detection optics from the *c*-axis of AlN. The relation between ϕ and the internal angle θ [as defined in Fig. 3(a)] for the *c*-plane AlN is derived by Snell's law assuming that the refractive index is 2.9 [26]. Figure 3(b) shows the θ-dependent PL spectra of the *c*-plane homoepitaxial AlN film at 10 K, where the peak intensities are normalized. At $\theta = 0°$, the experimental configuration is $(k \parallel c, E \perp c)$, where k is the Poynting vector of the luminescence signals. The $(k \perp c, E \parallel c)$ component increases with θ. The 6.0267-eV peak emission decreases while the 6.0306 and 6.0399 eV peaks increase as θ increases due to the selection rule described in the previous paragraph. Figure 3(b) also shows the PL spectrum of the *m*-plane bulk AlN (violet, dotted line) at 10 K. The *m*-plane bulk AlN was excited at an (external) angle of 60° from the surface normal, and the PL signal was detected from the surface normal. Thus, the experimental configuration is $k \perp c$ ($\phi = \theta = 90°$). Although the 6.0306 and 6.0399 eV peaks have the same optical polarization ($E \parallel c$), the 6.0306-eV peak disappears for $k \parallel c$ whereas the 6.0399-eV peak disappears for $k \perp c$ [Fig. 3(b)]. The results indicate that the 6.0306-eV peak is a transverse wave ($k \perp E$) with an irreducible representation of Γ_1 (hereafter, it is denoted as Γ_1^T), while the 6.0399-eV peak is a longitudinal wave ($k \parallel E$) with an irreducible representation of Γ_1 (hereafter, it is denoted as Γ_1^L). Hopfield *et al.* pointed out that longitudinal excitons are observable in uniaxial crystals due to the finite wave number of excitons [27]. It should be noted that we assigned the 6.0306-eV peak to the bound state of the 6.0399-eV peak [10,21]. We herein revise the assignment (a free transverse exciton with an irreducible representation of Γ_1).

Below, we interpret the experimental results. To date, the 1*s* excitonic effective Hamiltonian H with a 12×12 matrix has been used to describe the excitonic structure of GaN and AlN as

$$H = \Delta_1 J_z^2 + \Delta_2 J_z \sigma_{vz} + \Delta_3 (\sigma_{+v} J_- + \sigma_{-v} J_+) + \tfrac{1}{2} j_0 (\sigma_e \cdot \sigma_h),$$
(1)

where Δ_1, $\Delta_{2,3}$, and j_0 describe the crystal-field splitting, spin-orbit interaction, and short-range electron-hole exchange interaction, respectively [7,8,10,11,16]. J and σ describe the orbital angular momentum and Pauli-matrix operator, respectively [28]. However, this framework cannot explain angle-dependent PL emission energies. Figure 3(c) shows an expanded graph of Fig. 3(b), including the Lorentizian-fitted curves of the experimental PL spectra. An emission energy (left dotted line) depends on the detection angle. Therefore,
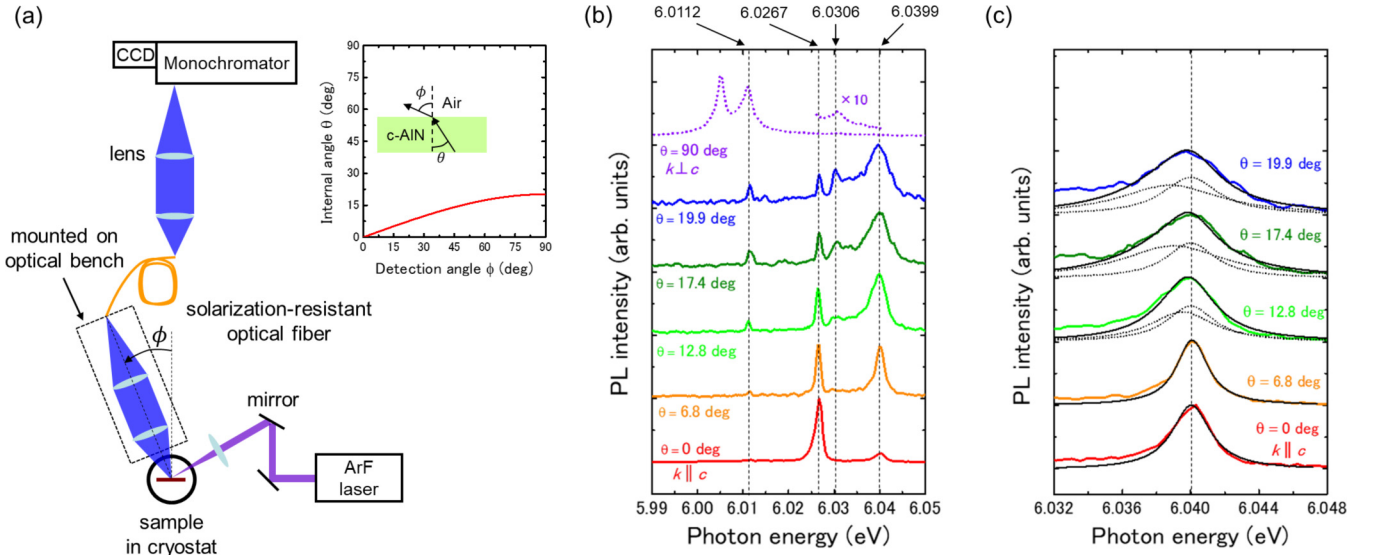
FIG. 3. (a) Experimental setup for angle-resolved PL spectroscopy. Relation between the detection (external) angle ϕ and the internal angle θ for c-plane AlN is also shown. (b) Angle-resolved PL spectra of a c-plane homoepitaxial AlN film and an m-plane bulk AlN (violet, dotted line) at 10 K. $\theta = 0°$ corresponds to the ordinary-ray configuration. The excitation power density is 63 kW/cm^2. The 6.0306-eV peak disappears for $k \parallel c$ whereas the 6.0399-eV peak disappears for $k \perp c$. (c) Expanded graph of Fig. 3(b). The peak intensities are normalized. Black solid lines are Lorentzian-fitted curves while black dotted lines represent the spectral component (two Lorentzian fitting). An emission energy (left dotted line) depends on the detection angle.

we propose adding a long-range electron-hole exchange interaction [29] to Eq. (1). Because the A exciton in AlN is energetically decoupled from the B and C excitons by the strong crystal-field splitting [11], their mixing can be neglected. Within this approximation, the four A exciton energies, E_{Γ_1}, E_{Γ_2}, and E_{Γ_5}, can be written as

$$E_{\Gamma_5} = E_{\Gamma_2}, \tag{2}$$

$$E_{\Gamma_1}(\theta) = E_{\Gamma_5} + 2(j_0 + j_1 \cos^2 \theta), \tag{3}$$

where j_1 is the long-range electron-hole exchange interaction constant [29]. In AlN, Eq. (2) shows that the energy of the A exciton with an irreducible representation of Γ_5 is independent of θ because of the tiny oscillator strength, while Eq. (3) indicates that the energy of the A exciton with an irreducible representation of Γ_1 has an angle-dependent energy due to the large oscillator strength. According to our experimental results, $E_{\Gamma_1}(\theta = 0°)$ (that is Γ_1^L) and $E_{\Gamma_1}(\theta = 90°)$ (that is Γ_1^T) have energies of 6.0399 and 6.0306 eV, respectively. Consequently, j_0 and j_1 are derived as $+1.95$ and $+4.65$ meV, respectively. Table I summarizes the θ dependence of E_{Γ_1}. The experimental data for semipolar AlN films [21] are also taken. E_{Γ_1} is deduced by the Lorentzian fitting of the experimental PL spectra. Figure 4 shows the experimental and calculated θ-dependences of the A exciton energies in AlN at the Γ point at 10 K. Our theoretical framework fully explains the angle-dependent experimental results. It also solves the problem [16] where nonpolar and semipolar AlN samples exhibit lower PL peak energies (the luminescence signals were detected from the surface normal) compared to those for c-plane AlN samples. Figures 3(b) and 3(c) show the background emissions between 6.0306 and 6.0399 eV at $\theta \neq 0°$ and $90°$, which are attributed to the complexed upper/lower branch of

the mixed mode exciton-polariton [30] in AlN. However, this finite wave-vector effect is beyond the scope of this paper.

Finally, we compared the present results to those in previous studies. The luminescence properties of an m-plane homoepitaxial AlN film with relatively low impurity concentrations were studied [15,19]. The Γ_1^T (denoted as $\omega_A^L(\Gamma_5)$ and $\Gamma_1^{n=1}$ in Refs. [15] and [19], respectively) peak exhibits a stronger emission than the Γ_1^L (denoted as FX$_A(\Gamma_1)$ and $\Gamma_5^{n=1}$ in Refs. [15] and [19], respectively) peak, for the $k \perp c$ configuration [34]. The experimental results are consistent with ours, indicating that the relatively higher impurity concentrations of our m-plane bulk AlN do not affect the findings in this paper. It should be noted that although the experimental results are consistent, our assignment differs from that in the previous studies [15,19]. Table II shows the singlet-triplet Δ_{st} and longitudinal-transverse Δ_{LT} splitting energies of the energetically lowest exciton for select wide band-gap materials. Because Δ_{LT} is proportional to the oscillator strength

TABLE I. θ versus E_{Γ_1}. E_{Γ_1} is deduced by the Lorentzian fitting of the experimental PL spectra.

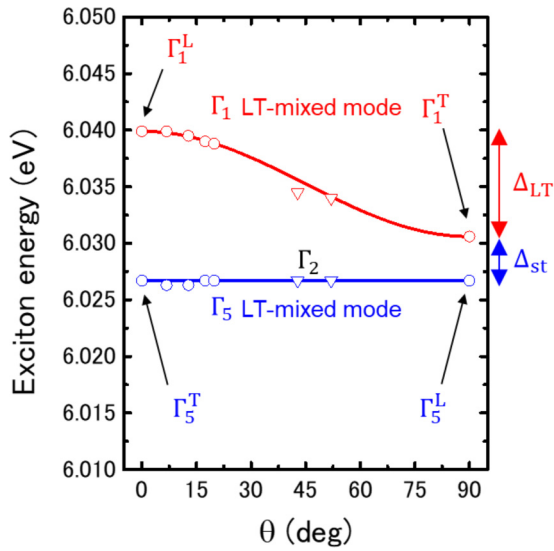| θ (degree)	E_{Γ_1} (eV)
0 (This work)	6.0399
6.8 (This work)	6.0399
12.8 (This work)	6.0395
17.4 (This work)	6.0390
19.9 (This work)	6.0388
42.8 (Ref. [21])	6.0345
52.0 (Ref. [21])	6.0340
90 (This work)	6.0306

FIG. 4. Internal angle θ dependence of the A exciton energy of AlN at the Γ point at 10 K. Lines are the calculated results. Circular and triangular points are the experimental results in this study and Ref. [21], respectively. Δ_{st} and Δ_{LT} are the singlet-triplet and longitudinal-transverse splitting energies, respectively.

TABLE II. Singlet-triplet Δ_{st} and longitudinal-transverse Δ_{LT} splitting energy of the energetically lowest exciton in wide band-gap materials.

Materials	Δ_{st} (meV)	Δ_{LT} (meV)
CuBr (Ref. [31])	1.7	12.2
CuCl (Ref. [31])	2.5	5.5
CdS (Ref. [31])	0.2	1.8
ZnTe (Ref. [31])	0.1	0.7
ZnO (Ref. [31])	0.17	2.16
ZnO (Ref. [32])	-	1.97
GaN (Ref. [33])	0.12	1.0
AlN (This work)	3.9	9.3

The valence band ordering in ZnO is out of the scope of this paper [32,37,38].

In conclusion, polarization- and angle-resolved PL spectroscopies are performed for AlN. All the experimental results, including previously reported ones, are readily explained by assigning the positive short-range and long-range electron-hole exchange interaction constants as $j_0 = 1.95$ meV and $j_1 = 4.65$ meV, respectively. The large Δ_{LT} suggests strong light–matter coupling in AlN.

of excitons [35], Table II suggests that strong light-matter coupling occurs in bulk AlN. AlN is a promising material for highly efficient DUV emitters. The small Δ_{LT} in ZnO is due to strong valence band mixing. The Δ_{LT} of the B and C excitons are reported to be around 10 meV in ZnO [32,36].

[1] M. Kneissl, T. Seong, J. Han, and H. Amano, Nat. Photon. **13**, 233 (2019).

[2] D. Welch, M. Buonanno, V. Grilj, I. Shuryak, C. Crickmore, A. W. Bigelow, G. Randers-Pehrson, G. W. Johnson, and D. J. Brenner, Sci. Rep. **8**, 2752 (2018).

[3] R. Ishii, M. Funato, and Y. Kawakami, APL Photon. **4**, 070801 (2019).

[4] Z. Zhang, M. Kushimoto, T. Sakai, N. Sugiyama, L. J. Schowalter, C. Sasaoka, and H. Amano, Appl. Phys. Express **12**, 124003 (2019).

[5] Y. Narukawa, M. Ichikawa, D. Sanga, M. Sano, and T. Mukai, J. Phys. D: Appl. Phys. **43**, 354002 (2010).

[6] A. Shikanai, T. Azuhata, T. Sota, S. F. Chichibu, A. Kuramata, K. Horino, and S. Nakamura, J. Appl. Phys. **81**, 417 (1997).

[7] B. Gil and O. Briot, Phys. Rev. B **55**, 2530 (1997).

[8] R. Ishii, A. Kaneta, M. Funato, Y. Kawakami, and A. A. Yamaguchi, Phys. Rev. B **81**, 155202 (2010).

[9] B. Neuschl, K. Thonke, M. Feneberg, S. Mita, J. Xie, R. Dalmau, R. Collazo, and Z. Sitar, Phys. Stat. Sol. (b) **249**, 511 (2012).

[10] R. Ishii, M. Funato, and Y. Kawakami, Phys. Rev. B **87**, 161204(R) (2013).

[11] R. Ishii, A. Kaneta, M. Funato, and Y. Kawakami, Phys. Rev. B **87**, 235201 (2013).

[12] M. Kaneko, H. Okumura, R. Ishii, M. Funato, Y. Kawakami, T. Kimoto, and J. Suda, Appl. Phys. Express **6**, 062604 (2013).

[13] S. F. Chichibu, K. Hazu, Y. Ishikawa, M. Tashiro, T. Ohtomo, K. Furusawa, A. Uedono, S. Mita, J. Xie, R. Collazo, and Z. Sitar, Appl. Phys. Lett. **103**, 142103 (2013).

[14] R. Ishii, M. Funato, and Y. Kawakami, Jpn. J. Appl. Phys. **53**, 091001 (2014).

[15] S. F. Chichibu, K. Kojima, K. Hazu, Y. Ishikawa, K. Furusawa, S. Mita, R. Collazo, Z. Sitar, and A. Uedono, Appl. Phys. Lett. **115**, 151903 (2019).

[16] M. Feneberg, M. Romero, B. Neuschl, K. Thonke, M. Röppischer, C. Cobet, N. Esser, M. Bickermann, and R. Goldhahn, Appl. Phys. Lett. **102**, 052112 (2013).

[17] C. Reich, M. Feneberg, V. Kueller, A. Knauer, T. Wernicke, J. Schlegel, M. Frentrup, R. Goldhahn, M. Weyers, and M. Kneissl, Appl. Phys. Lett. **103**, 212108 (2013).

[18] B. Neuschl, K. Thonke, M. Feneberg, R. Goldhahn, T. Wunderer, Z. Yang, N. M. Johnson, J. Xie, S. Mita, A. Rice, R. Collazo, and Z. Sitar, Appl. Phys. Lett. **103**, 122105 (2013).

[19] Z. Bryan, I. Bryan, M. Bobea, L. Hussey, R. Kirste, Z. Sitar, and R. Collazo, J. Appl. Phys. **115**, 133503 (2014).

[20] I. Bryan, Z. Bryan, M. Bobea, L. Hussey, R. Kirste, R. Collazo, and Z. Sitar, J. Appl. Phys. **116**, 133517 (2014).

[21] S. Ichikawa, M. Funato, and Y. Kawakami, J. Cryst. Growth **522**, 68 (2019).

[22] M. Funato, K. Matsuda, R. G. Banal, R. Ishii, and Y. Kawakami, Appl. Phys. Express **5**, 082001 (2012).

[23] Q. Yan, P. Rinke, M. Winkelnkemper, A. Qteish, D. Bimberg, M. Scheffler, and C. G. Van de Walle, Semicond. Sci. Technol. **26**, 014037 (2011).

[24] H. Ikeda, T. Okamura, K. Matsukawa, T. Sota, M. Sugawara, T. Hoshi, P. Cantu, R. Sharma, J. F. Kaeding, S. Keller, U. K. Mishra, K. Kosaka, K. Asai, S. Sumiya, T. Shibata, M. Tanaka, J. S. Speck, S. P. DenBaars, S. Nakamura, T. Koyama, T. Onuma, and S. F. Chichibu, J. Appl. Phys. **102**, 123707 (2007).

[25] B. Gil, D. Felbacq, B. Guizal, and G. Bouchitté, Phys. Stat. Sol. (b) **249**, 455 (2012).

[26] M. Feneberg, M. F. Romero, M. Röppischer, C. Cobet, N. Esser, B. Neuschl, K. Thonke, M. Bickermann, and R. Goldhahn, Phys. Rev. B **87**, 235209 (2013).

[27] J. J. Hopfield and D. G. Thomas, J. Phys. Chem. Solids **12**, 276 (1960).

[28] D. W. Langer, R. N. Euwema, K. Era, and T. Koda, Phys. Rev. B **2**, 4005 (1970).

[29] K. Cho, Phys. Rev. B **14**, 4463 (1976).

[30] R. Kuhnert, R. Helbig, and K. Hümmer, Phys. Stat. Sol. (b) **107**, 83 (1981).

[31] B. Hönerlage, R. Levy, J. B. Grun, C. Klingshirn, and K. Bohnert, Phys. Rep. **124**, 161 (1985).

[32] M. R. Wagner, G. Callsen, J. S. Reparaz, R. Kirste, A. Hoffmann, A. V. Rodina, A. Schleife, F. Bechstedt, and M. R. Phillips, Phys. Rev. B **88**, 235210 (2013).

[33] A. V. Rodina, M. Dietrich, A. Göldner, L. Eckey, A. Hoffmann, A. L. Efros, M. Rosen, and B. K. Meyer, Phys. Rev. B **64**, 115204 (2001).

[34] In Ref. [19], PL signals were detected at an angle of 45° from the surface normal (*m*-plane). Considering Snell's law [see Fig. 3(a)], the configuration corresponds to almost $k \perp c$.

[35] T. Oshikiri and Y. Onodera, J. Phys. Soc. Jpn. **51**, 2194 (1982).

[36] S. F. Chichibu, T. Sota, G. Cantwell, D. B. Eason, and C. W. Litton, J. Appl. Phys. **93**, 756 (2003).

[37] M. R. Wagner, J. H. Schulze, R. Kirste, M. Cobet, A. Hoffmann, C. Rauch, A. V. Rodina, B. K. Meyer, U. Röder, and K. Thonke, Phys. Rev. B **80**, 205203 (2009).

[38] A. Takagi, A. Nakamura, A. Yoshikaie, S. Yoshioka, S. Adachi, S. F. Chichibu, and T. Sota, J. Phys.: Condens. Matter **24**, 415801 (2012).